Proceedings of the DIS'2004, Štrbské Pleso, Slovakia

DIFFRACTIVE MEASUREMENTS AT CDF

KOJI TERASHI
(FOR THE CDF COLLABORATION)
The Rockefeller University
1230 York Avenue, New York, NY 10021, USA
E-mail: terashi@rockefeller.edu

We present results on the measurements of the diffractive structure function and exclusive final states obtained by the CDF Collaboration in proton-antiproton collisions at the Fermilab Tevatron.

1 Introduction : Overview of Run I Results

Diffractive events in $\bar{p}p$ collisions are characterized by the presence of a leading proton or antiproton which remains intact, and/or a rapidity gap, defined as a pseudorapidity[a] region devoid of particles. Diffractive events involving hard processes ("hard diffraction"), such as production of high E_T jets (see Fig. 1), have been studied extensively to understand the nature of the exchanged object, the Pomeron, which in QCD is a color singlet entity with vacuum quantum numbers. One of the most interesting questions in hard diffractive processes is whether or not they obey QCD factorization, in other words, whether the Pomeron has a universal, process independent, parton distribution function (PDF). Results on diffractive deep inelastic scattering (DDIS) from the ep collider HERA show that QCD factorization holds in DDIS. However, single diffractive (SD) rates of W-boson [1], dijet [2], b-quark [3] and J/ψ [4] production relative to non-diffractive (ND) ones measured in Run I at CDF are $\mathcal{O}(10)$ lower than expectations from PDFs determined at HERA, and it indicates a severe breakdown of QCD factorization in hard diffraction between Tevatron and HERA. The suppression factor at the Tevatron relative to HERA is approximately equal in magnitude to that measured in soft diffraction cross sections relative to Regge theory predictions based on Regge factorization.

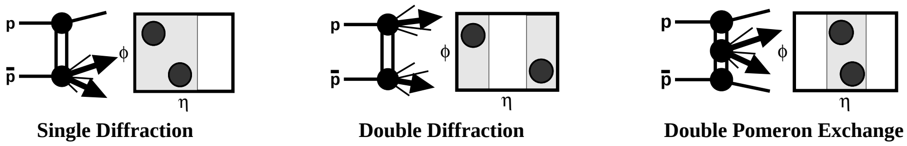

Figure 1. Diagrams and event topologies of dijet production in single diffraction (left), double diffraction (middle) and double pomeron exchange (right).

[a] The pseudorapidity η of a particle is defined as $\eta \equiv -\ln(\tan\theta/2)$, where θ is the polar angle of the particle with respect to the proton beam direction.

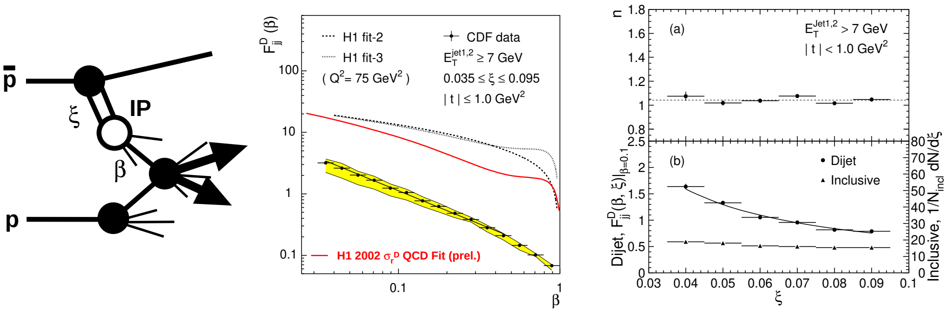

Figure 2. Left: Diagram of diffractive dijet production. Center: Data β distribution (points) compared with expectations from DDIS at H1 (curves). The straight line on the data is a fit of the form β^{-n}. Right: Distributions versus ξ: (a) the parameter n of a fit to the F_{jj}^D of the form $F_{jj}^D(\beta,\xi)|_\xi = C\beta^{-n}$ for $\beta < 0.5$; (b) the F_{jj}^D at $\beta = 0.1$ fitted to the form $F_{jj}^D(\beta,\xi)|_{\beta=0.1} = C\xi^{-m}$ (circle-points and curve), and the inclusive SD distribution (triangles).

The suppression relative to predictions based on DDIS PDFs is illustrated in Fig. 2, which shows the "diffractive structure function" F_{jj}^D measured at CDF by using diffractive dijet data with a leading antiproton detected in Roman Pots [5] [6]. The analysis was performed using inclusive Roman Pot trigger data in the kinematic range of $0.035 < \xi < 0.095$ and $|t| < 1.0$ GeV^2 and selecting events with dijets of $E_T^{jet} > 7$ GeV, where ξ is the fractional momentum loss of the antiproton and t is the four momentum transfer squared. The $\tilde{F}_{jj}^D$ (integrated over E_T^{jet}, ξ and t) was obtained as a function of β, momentum fraction of the parton in the Pomeron given by $\beta = x_{\bar{p}}/\xi$ ($x_{\bar{p}}$ is x-Bjorken of the parton in the antiproton, see Fig. 2), by measuring the ratio of diffractive to non-diffractive dijet rates and using the known leading order PDFs of the proton. The measured suppression of F_{jj}^D relative to expectations from the H1 PDFs is approximately equal to that observed in soft diffraction. Also shown in Fig. 2 is ξ and β dependence of the F_{jj}^D in diffractive dijets. The F_{jj}^D turned out to be well represented by the β-ξ factorisable form;

$$F_{jj}^D(\beta,\xi) = C \cdot \beta^{-n} \cdot \xi^{-m} \tag{1}$$

in the region $\beta < 0.5$ and $0.035 < \xi < 0.095$, where $n = 1.0 \pm 0.1$ and $m = 0.9 \pm 0.1$. The measured $\xi^{-0.9\pm0.1}$ dependence of F_{jj}^D indicates that the diffractive dijet sample is dominated by Pomeron exchange, which has a $\xi^{-\alpha(0)} \approx \xi^{-1.1}$ dependence, where $\alpha(0)$ is the value of Pomeron trajectory $\alpha(t)$ at $t = 0$.

CDF has also studied dijet events with a double Pomeron exchange (DPE) topology (Fig. 1) using the Roman Pot trigger sample at $\sqrt{s} = 1800$ GeV [7]. For dijets with $7 < E_T^{jet1,2} < 10$ GeV in the region $0.035 < \xi_{\bar{p}} < 0.095$ and $|t_{\bar{p}}| < 1.0$ GeV^2 and for DPE $0.01 < \xi_p < 0.03$, the ratio of DPE to SD dijet rates (R_{SD}^{DPE}) was compared with that of SD to ND rates (R_{ND}^{SD}), where the subscript $\bar{p}$ (p) in $\xi_{\bar{p}}$ and $t_{\bar{p}}$ (ξ_p) denotes that the quantity is for the antiproton (proton). Fig. 3 shows the measured R_{SD}^{DPE} and R_{ND}^{SD} as a function of x-Bjorken of partons in the proton and antiproton, respectively. The comparison of the two ratios was done at fixed x-Bjorken (denoted by vertical dashed lines in the figure) and $\xi = 0.02$

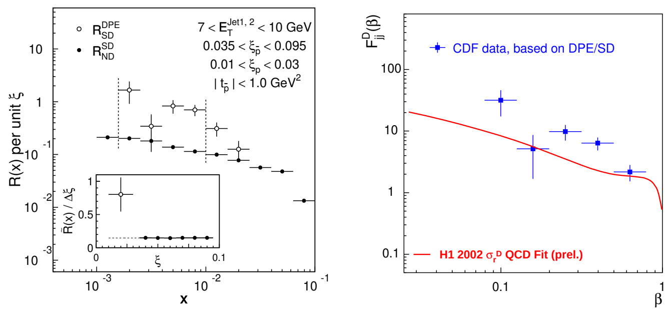

Figure 3. Left: Ratio of DPE to SD (SD to ND) dijet event rates per unit ξ_p ($\xi_{\bar{p}}$), shown as open (solid) circles, as a function of x-Bjorken of partons in the (anti)proton. The errors are statistical only. The inset shows SD to ND ratio (weighted average of the ratio in the region of x within the vertical dashed lines) versus ξ per unit ξ. Right: β distribution (points) obtained from the DPE to SD ratio, compared with expectations from DDIS at H1 (curve).

by extrapolating a straight line fit obtained from the R^{SD}_{ND} points in the range $0.035 < \xi < 0.095$, in which a flat ξ behavior is seen. A breakdown of factorization was observed in the ratio comparison and the discrepancy was measured to be $D = R^{SD}_{ND}/R^{DPE}_{SD} = 0.19 \pm 0.07$.

The F^D_{jj} of the proton was also measured using the R^{DPE}_{SD} ratio (Fig. 3) and compared with expectation from the H1 PDFs. Here the expectation was re-calculated at fixed $\xi = 0.02$. Given that a normalization systematic uncertainty of the R^{DPE}_{SD} ratio is about $\pm 25\%$, the F^D_{jj} measured from DPE dijets appears to be approximately equal to the expectation from H1 DDIS. This indicates that the formation of a second rapidity gap is unsuppressed in events which have a gap on the other side.

2 Run II Diffraction Measurements

In Run II, being currently under way, CDF plans to study various topics on diffraction, including Q^2 and ξ dependence of F^D_{jj} in SD, gap width dependence of F^D_{jj} in DPE, production of exclusive dijet, heavy flavor and low mass states in DPE, and dijets with a large gap in-between jets. Two recently installed "Miniplug" (MP) calorimeters cover the region $3.5 < |\eta| < 5.1$, and 7 stations of scintillation counters, called Beam Shower Counters (BSC), mounted around the beam pipe, extend the coverage to the very forward region of $5.5 < |\eta| < 7.5$. The Roman Pots (RP) used in Run I were re-installed and are being operated to trigger on leading antiprotons in the kinematic range $0.02 < \xi < 0.1$ and $0 < |t| < 2$ GeV^2.

3 Diffractive Dijet Production in Run II

Triggering on a leading antiproton in the RP in conjunction with at least one calorimeter tower with $E_T > 5$ GeV (RP+ST5 trigger), a study of diffractive dijet events has been performed. From a sample of 352K triggered events, about 15K

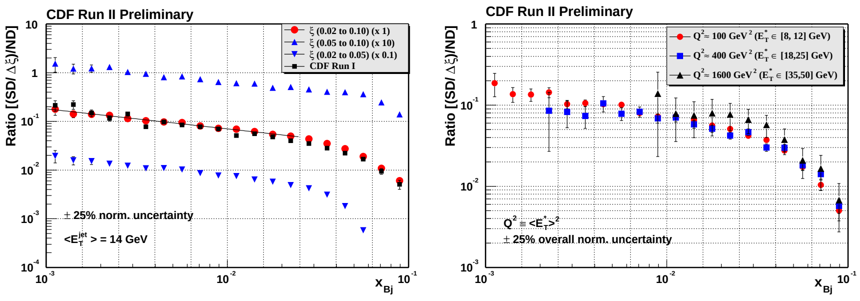

Figure 4. Ratio of SD to ND dijet rates per unit ξ as a function of x-Bjorken of the parton in the antiproton. Left: ratios for different ξ intervals; $0.02 < \xi < 0.1$ (circles), $0.02 < \xi < 0.05$ (downward triangles) and $0.05 < \xi < 0.1$ (upward triangles) for average dijet E_T of 14 GeV, compared with Run I measurement (squares). Right: ratios for different E_T^* (average jet E_T) intervals; $8 < E_T^* < 12$ GeV (circles), $18 < E_T^* < 25$ GeV (squares) and $35 < E_T^* < 50$ GeV (triangles). The Q^2 in the plot is defined as $Q^2 = \langle E_T^* \rangle^2$.

SD dijet events with dijets of corrected $E_T > 5$ GeV in the range $0.02 < \xi < 0.1$ were obtained. The value of ξ (fractional momentum loss of the antiproton) was calculated by summing up energies in all calorimeter towers including MP as follows,

$$\xi = \frac{\sum_i E_T^i e^{-\eta_i}}{\sqrt{s}}. \tag{2}$$

Using a non-diffractive dijet sample triggered on the same calorimeter tower requirement, the ratio of diffractive to non-diffractive dijet rates was measured as a function of x-Bjorken of the parton in the antiproton, as shown in Fig. 4. This figure shows that (i) the ratio observed with Run II data in approximately the same kinematic region as in Run I data is consistent with Run I results, and (ii) there is no appreciable ξ dependence in the ratio, as already seen in Run I. Measurement of the ξ dependence at lower ξ values ($\xi < 0.02$) is one of our Run II goals and is being currently under study. Another interesting observation of the ratio is its Q^2 dependence, which would tell us QCD evolution of the Pomeron. Preliminary results of the Q^2 dependence of the ratio, where Q^2 is defined as the square of average value of the mean dijet E_T, are shown in Fig. 4. In the range $100 < Q^2 < 1600$ GeV^2 no significant Q^2 dependence has been observed, and it indicates that the Pomeron could evolve with Q^2 in a similar way as the proton.

4 Dijet Production by Double Pomeron Exchange in Run II

In Run I we observed dijet events with a double Pomeron exchange topology by looking for a rapidity gap in the beam-beam counter and forward calorimeter towers in the outgoing proton direction. Similarly, in Run II we observed DPE dijet signal as an enhancement of events with a rapidity gap on the proton-side in the two-dimensional LEGO plot of MP versus BSC hit multiplicity of SD dijet events (Fig. 5). For a detailed study of DPE dijets, we have implemented a dedicated trigger that requires a BSC gap on the proton-side, in addition to the requirements

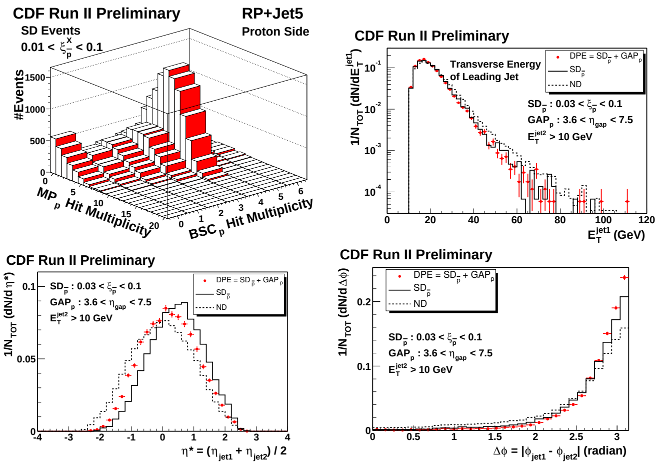

Figure 5. MP hit multiplicity versus BSC hit counter multiplicity on the proton-side in SD dijet sample (top left). E_T distributions of the leading jet (top right), mean η (bottom left) and $\Delta\phi$ (bottom right) of the two leading jets in DPE dijet events (points) compared with those of the SD (solid histogram) and ND (dashed histogram) dijet samples. All three distributions are normalized per unit area.

for RP+ST5 trigger (e.g, leading antiproton in the RP and a single calorimeter tower of $E_T > 5$ GeV). Requiring offline an addition gap in the MP on the proton-side, we obtained about 16K dijet events (about 100 times more data than in Run I), which are qualitatively consistent with DPE dijets. Figure 5 shows the E_T of the leading jet, mean η and azimuthal angle difference $\Delta\phi$ of the two leading jets for the DPE dijet events. As seen in Run I DPE data, the E_T distributions look similar to those of SD dijets (histograms), while the mean η and $\Delta\phi$ show that the DPE dijets are more central and more back-to-back.

For those 16K DPE dijet candidate events, we examined "dijet mass fraction", R_{jj}, defined as the invariant mass M_{jj} of the two leading jets divided by the mass M_X of the whole system (except leading nucleons);

$$R_{jj} = M_{jj}/M_X. \tag{3}$$

This observable should be sensitive to how much the event energy is concentrated in the dijet. The system mass M_X was obtained from the values of ξ in an event by $M_X = \sqrt{\xi_p \cdot \xi_{\bar{p}} \cdot s}$ and the ξ values were calculated as above from all calorimeter towers. The dijet mass M_{jj} was obtained from the calorimeter tower energies inside the R=0.7 cones of jets. In principle, if the dijet is produced exclusively and there is no leak of jet energy from the cones, the ratio R_{jj} should be one. Fig. 6 shows the distributions of M_{jj} and R_{jj} for DPE dijets, compared with those for SD dijets. DPE and SD dijets have the similar M_{jj}, while the DPE has a higher R_{jj} value because the DPE has much smaller M_X (due to the proton-side gap). There are quite a few DPE events at very high R_{jj} (say, > 0.8), but the curve appears to be falling very smoothly as $R_{jj} \to 1$, that could indicate the presence of a large "tail" of inclusive background at high R_{jj}. Given that the exclusive dijet production is

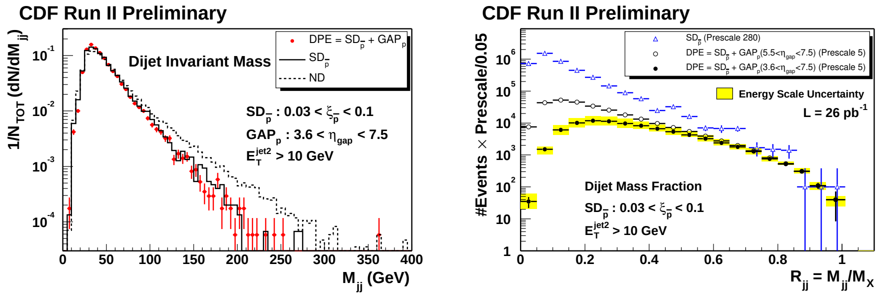

Figure 6. Left: Invariant mass of two leading jets in DPE dijet events (points) compared with those of the SD (solid histogram) and ND (dashed histogram) dijet samples. Right: Distributions of dijet mass fraction (see text) for SD (triangles) dijets and DPE dijets with a gap in the range $3.6 < \eta < 7.5$ (solid circle-points) or $5.5 < \eta < 7.5$ (open circle-points). The distributions are corrected for prescale factors in the triggers and normalized to the same luminosity (26 pb^{-1}).

expected at $R_{jj} > 0.8$ or so, we obtained the cross sections of events with $R_{jj} > 0.8$, as the upper limits of exclusive dijet production, to be $970 \pm 65(\text{stat}) \pm 272(\text{syst})$ pb and $34 \pm 5(\text{stat}) \pm 10(\text{syst})$ pb for the leading jet $E_T > 10$ and > 25 GeV, respectively, in events with a gap in the region $3.6 < \eta_{gap} < 7.5$, $0.03 < \xi_{\bar{p}} < 0.1$ and dijets of $|\eta^{jet}| < 2.5$. The cross section for $E_T^{jet1} > 25$ GeV is consistent with a prediction for exclusive dijet production from Khoze, Martin and Ryskin (KMR) [8], that is ~ 60 pb with factor 2 uncertainty for dijets of $25 < E_T^{jet} < 35$ GeV and $|\eta^{jet1} - \eta^{jet2}| < 2$.

5 Exclusive χ_c Search in Run II

Observing Higgs boson is one of the main goals at the Tevatron and future LHC colliders. Current limits of the Standard Model (SM) Higgs boson seems to prefer relatively light mass ($M_{Higgs} \sim 120$ GeV). However, observing the light SM Higgs which predominantly decays to $b\bar{b}$ in conventional inclusive processes is known to be very difficult due to huge QCD $b\bar{b}$ background. "Exclusive Higgs production" originally discussed in Ref. [9] is now considered to be a possible way of observing light SM Higgs. The process goes through gluon-gluon fusion via top quark loop ($gg \to [t-\text{loop}] \to H$) while the second *soft* gluon is exchanged between the p and $\bar{p}$ to screen the color flow. The final state of the event contains therefore only Higgs boson and very forward leading nucleons. Exclusive processes in other final states have been studied theoretically, and exclusive $\chi_{c(b)}$ meson is known to be a benchmark process to look for exclusive Higgs because of the similarity of the predominant process of exclusive χ production; $gg \to [c(b) - \text{loop}] \to \chi_{c(b)}$. KMR predicts that the cross section of exclusive χ_c^0 production at the Tevatron is about 600 nb [10][b].

[b] Exclusive χ_b^0 production cross section at the Tevatron is expected to be very small ($3 \sim 4$ orders of magnitude lower than exclusive χ_c^0 cross section) and the branching fraction of $\chi_b^0 \to \Upsilon\gamma$ decay, which is suited for the experimental search, is unknown so far

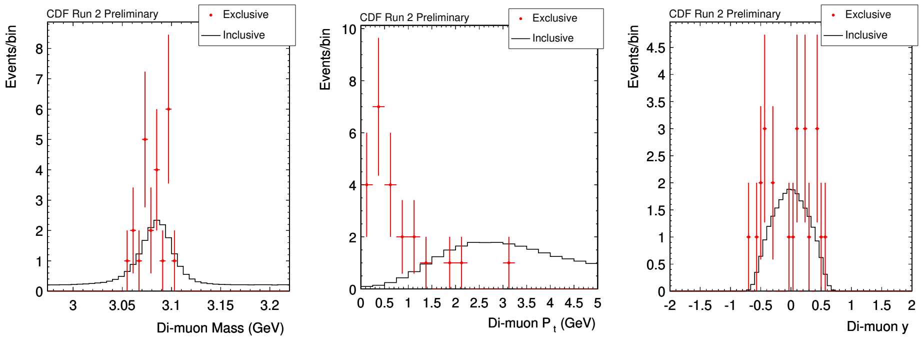

Figure 7. Invariant mass (left), transverse momentum (middle) and rapidity (right) of the dimuon in the exclusive J/ψ candidate events (points), compared with those of inclusive events (histogram).

Search for exclusive χ_c^0 meson production was performed in CDF using Run II data. About 93 pb^{-1} of inclusive J/ψ ($\rightarrow \mu\mu$) trigger data that requires two muons with $p_T^\mu > 1.5$ GeV/c, $|\eta_\mu| < 0.6$ and the invariant mass of the muon pair in the J/ψ mass window was used in the analysis. After rejecting cosmic background using the time-of-flight detector information, rapidity gaps were required in the BSC and MP on the both side to select J/ψ events in DPE. Observing 107 DPE J/ψ events and further requiring large rapidity gaps in the plug and central regions, 23 exclusive candidate events were found with the dimuon invariant mass in the J/ψ mass peak, 10 of which contained only one electromagnetic tower that appeared to be a photon candidate. Fig. 7 shows the invariant mass, p_T and η of the dimuon in the 23 exclusive candidate events, compared with the distributions in the inclusive J/ψ sample.

For those 10 events with a photon candidate electromagnetic tower, the invariant mass of the dimuon and the photon is shown in Fig. 8. The mass of the dimuon-photon system appears to be consistent with prediction from Monte Carlo for the exclusive χ_c^0 production. Assuming that those 10 events are all exclusive $J/\psi + \gamma$ events, we obtained the cross section of exclusive $J/\psi + \gamma$ production to be $49 \pm 18(\text{stat}) \pm 39(\text{syst})$ pb. This cross section can be used as the upper limit of exclusive χ_c^0 (decaying to $J/\psi + \gamma$) production cross section. From the KMR prediction of exclusive χ_c^0 production (600 nb), we expect the cross section of exclusive $\chi_c^0 \rightarrow J/\psi + \gamma$ to be about 70 pb for the J/ψ rapidity range of $|y^{J/\psi}| < 0.6$. The measured cross section is consistent with the KMR prediction.

6 Prospects of Diffractive Physics in Run II

Measurements of Q^2 and ξ dependence of diffractive structure function F_{jj}^D in SD dijets are very important. We observed no ξ dependence in SD to ND dijet event rates in the range $0.03 < \xi < 0.1$ (confirming Run I results). New Run II data from "Gap + Jet" trigger which requires a BSC gap and jets in an event will allow us to extend the ξ range down to possibly $\xi \sim 0.001$ for $Q^2 > 100$ GeV^2.

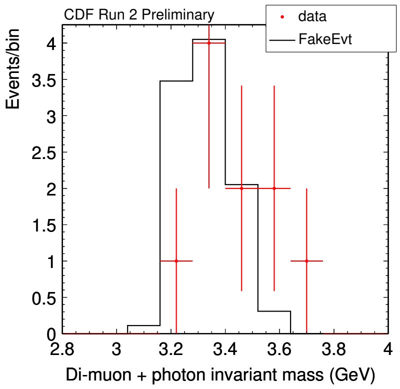

Figure 8. Invariant mass of the system of the dimuon and a photon in 10 exclusive $J/\psi + \gamma$ candidate events (points), compared with prediction from exclusive χ_c^0 signal Monte Carlo (histogram).

Preliminary results of Q^2 dependence of SD to ND dijet rates indicates that there is no appreciable Q^2 dependence in the range $100 < Q^2 < 1600$ GeV^2. Using "RP + Jet20 (50)" trigger data that requires RP tag of leading $\bar{p}$ and jets with $E_T > 20$ (50) GeV, we will be able to explore the Q^2 range up to $\sim 10^4$ GeV^2.

Establishing exclusive production processes of dijets, χ_c^0 and diphoton experimentally (if they exist) is one of the goals in Run II. We are now developing new triggers for $b\bar{b}$, χ_c^0 and $\gamma\gamma$ productions in DPE to search for the exclusive processes. Contrary to χ_c^0 or $\gamma\gamma$, exclusive $b\bar{b}$ production is severely suppressed by "$J_Z = 0$ spin selection rule" for the gluon polarization. Therefore, we might be able to find exclusive "gg" jets in inclusive DPE dijets normalized to the $b\bar{b}$ jet spectrum. Constraints obtained on those exclusive processes at the Tevatron will be useful to calibrate predictions for exclusive Higgs production at the LHC.

References

1. F. Abe *et al.*, Phys. Rev. Lett. **78**, 2698 (1997).
2. F. Abe *et al.*, Phys. Rev. Lett. **79**, 2636 (1997).
3. T. Affolder *et al.*, Phys. Rev. Lett. **84**, 232 (2000).
4. T. Affolder *et al.*, Phys. Rev. Lett. **87**, 241802 (2001).
5. T. Affolder *et al.*, Phys. Rev. Lett. **84**, 5043 (2000).
6. T. Acosta *et al.*, Phys. Rev. Lett. **88**, 151802 (2002).
7. T. Affolder *et al.*, Phys. Rev. Lett. **85**, 4215 (2000).
8. V.A. Khoze, A.D. Martin, and M.G. Ryskin, Eur. Phys. J. C**23**, 311 (2002).
9. A. Bialas and P.V. Landshoff, Phys. Lett. B **256**, 540 (1991); A. Schäfer, O. Nachtmass and R. Schöpf, Phys. Lett. B **249**, 331 (1990); A. Bialas and W. Szeremeta, Phys. Lett. B **296**, 191 (1992).
10. V.A. Khoze, A.D. Martin, and M.G. Ryskin, Eur. Phys. J. C**19**, 477 (2001).